



Optimal electric bus fleet scheduling for a route with charging facility sharing

Jinhua Ji, Yiming Bie*, Linhong Wang*

School of Transportation, Jilin University, Changchun 130022, China



ARTICLE INFO

Keywords:

Electric bus
Vehicle scheduling
Charging facility sharing
Optimization model

ABSTRACT

To alleviate the shortage of charging facilities for electric cars (ECs) and increase the utilization rate of charging facilities for electric buses (EBs), we propose a charging facility sharing strategy that allows charging piles of EBs to be utilized by ECs for a fee during certain time windows. A nonlinear integer programming model is first developed with multiple objectives, including minimizing the average daily acquisition and charging costs of the EB route, minimizing the time costs for ECs waiting for charging, and maximizing the charging revenues from ECs, to collaboratively achieve the vehicle type allowed to be charged at each time window, daily service trips and charging trips allocated to each EB. Subsequently, an algorithm is developed to solve the formulated optimization model by combining the enumeration method and branch and price to address nonlinearity. Finally, a real EB route in Mehekou, Jilin Province, China, is taken as an example to verify the effectiveness of the proposed method. Results show that the charging facility sharing strategy can increase revenue for public transit companies and facilitate the charging of ECs without disrupting the timetable of EBs, which promises a win-win measure for both public transit companies and EC users.

1. Introduction

1.1. Background

Electric buses (EBs) produce zero emissions and low noise, and require simple driving operations compared to traditional fuel buses, which provides a new opportunity to reduce traffic emissions and save public transit company operating costs. In recent years, many countries have actively promoted the electrification of urban buses. For example, by the end of 2021, the size of the EB fleet in China had reached 419,500, accounting for 59.1% of the entire urban bus fleet. Among the nearly 75,000 buses deployed in the USA at the end of 2019, 450 were electric-powered. As of December 2020, over 2,700 EBs were delivered or ordered in the USA ([Global Mass Transit Report, 2021](#)). As of May 2020, 5,087 EBs had been delivered since 2012 in Europe, nearly 75% of them were handed over in 2019 and 2020 ([Sustainable Bus, 2020](#)).

While purchasing a large number of EBs, cities have also set up many charging facilities at depots/stations to meet their charging needs. During the day, however, most EBs are operating on routes that have relatively low charging demand, leaving charging piles unutilized mostly. Simultaneously, the growth in electric cars (ECs) in urban areas, along with limited public charging facilities, leads to a wide gap between charging demand and supply. According to data from the Ministry of Public Security of the People's Republic of

* Corresponding authors.

E-mail addresses: yimingbie@126.com (Y. Bie), wanghonglin0520@126.com (L. Wang).

China, as of June 2021, there are 4.93 million ECs but only 0.95 million public charging piles, implying that one public charging pile has to provide the service to up to 5.2 ECs on average. Consequently, ECs in cities usually suffer from long-time queuing before they can be charged. Under these circumstances, EB charging facilities being shared with ECs with a fee could be a feasible approach not only to alleviate the charging difficulties of ECs but also to increase the utilization rate of EB charging facilities as well as the charging revenues from ECs.

The charging facility sharing strategy allows the charging piles of EBs to be utilized by the ECs for a fee during certain periods. However, because of the occupation of charging piles by ECs, in-service EBs with insufficient power on the route may not be able to get charged in time, and public transit companies need to adjust the vehicle and charging scheduling schemes, which may cause an increase in operating costs (e.g., vehicle acquisition costs and electricity expenses). Therefore, it is a crucial task for public transit companies to collaboratively optimize the vehicle scheduling and charging facility sharing schemes, so as to maximize charging revenues from ECs while ensuring on-schedule operation.

1.2. Literature review

In recent years, many studies have been conducted on EB vehicle scheduling problems. Vehicle scheduling for buses is the process of assigning vehicles to trips on a given timetable, which is closely related to scheduling costs for operators (Ceder, 2011; Li, 2014; Teoh et al., 2018; Wang et al., 2020; Hu et al., 2022; Qu et al., 2022; Perumal et al., 2022; Meng et al., 2022; Zhang et al., 2022). In addition to trip assignment, vehicle scheduling for an EB route also needs to arrange charging trips for EBs (Abdelwahed et al., 2020; Bie et al., 2021a; Deng et al., 2021; Gkiotsalitis, 2021; Hall et al., 2019; Huang and Wang, 2022; Lajunen, 2014; Ma et al., 2021; Zhang et al., 2021). However, the arrangement of charging trips is significantly affected by the availability of charging facilities (Paul and Yamada, 2014; Li, 2016; Liu and Song, 2017; Pelletier et al., 2019; An, 2020; Liu et al., 2021a; Dirks et al., 2022; Coretti Sanchez et al., 2022; Yue et al., 2022). Existing studies on this topic can be roughly divided into two categories, according to the number of charging facilities.

(i) Vehicle scheduling for EBs with sufficient charging facilities

In this group, it was usually assumed that there were sufficient charging facilities for EBs, and the restriction of charging capacity on EB scheduling was not considered. Based on the remaining life additional benefit-cost, Li et al. (2018) developed an integer program to maximize the total net benefit of early replacement, where both the optimal fleet size and composition under budget constraints can be determined. Zhou et al. (2020) developed a bi-level programming model to collaboratively optimize vehicle scheduling and charging scheduling of a mixed bus fleet under the operating conditions of a single depot. Focusing on bus timetabling and vehicle scheduling for EBs, Teng et al. (2020) developed a multi-objective optimization model based on a particle swarm optimization algorithm. He et al. (2020) proposed a network modeling framework to optimize charging scheduling and charger deployment for a fast-charging system, which could minimize the total charging costs. Bie et al. (2021b) developed a vehicle scheduling method for the EB route, considering stochastic volatilities in trip travel time and energy consumption. Li et al. (2021) established an EB scheduling model with adjustable timetables for joint post-disaster distribution system restoration. Yildirim and Yildiz (2021) proposed an integer programming formulation to determine the optimal EB fleet composition and scheduling that could minimize the total procurement costs of the buses and the operating costs of the schedules. Huang et al. (2022) proposed a Lagrangian relaxation-based solution approach for the EB scheduling problem, which was formulated as a linear integer programming problem to minimize the total charging time. With the advent of modular autonomous vehicles, Liu et al. (2021b) presented an operational design for flex-route transit services, in which the vehicle scheduling problem was solved using customized dynamic programming with valid cuts.

(ii) Vehicle scheduling for EBs with limited charging facilities

In this group, the effects of the quantity, location, and power of charging facilities on EB scheduling are considered. Some studies have considered the parameters of charging facilities as decision variables and cooperatively optimized EB vehicle scheduling and charging facility deployment. For example, Wang et al. (2017) developed a modeling framework to optimize the location and capacity of charging stations while minimizing total annual costs. Leou and Hung (2017) proposed a mathematical model to determine the optimal contracted power capacity and charging schedule of an EB charging station to reduce the energy costs. Rogge et al. (2018) provided a methodology for the cost-optimized planning of depot charging battery bus fleets and their corresponding charging infrastructure. Li et al. (2020) proposed a joint optimization model for regular charging EB scheduling and stationary charger deployment, considering a partial charging policy and time-of-use electricity prices. Estrada et al. (2022) developed an operating model to estimate the number of EBs and charging facilities to be deployed in two charging schemes: charging at a bus garage facility and opportunity charging at on-street chargers. Wang et al. (2021) designed a pricing-aware real-time charging scheduling system based on the Markov decision process and a scheduling-based charging station upgrading strategy. Zhou et al. (2022) built a mixed-integer nonlinear and nonconvex programming model to determine the charger type and the vehicle and charging schedule.

In addition, in some studies, the deployment parameters of charging facilities were given and used as constraints for the development of optimal service and charging trip arrangement. Gao et al. (2018) proposed an optimal charging model with a fixed capacity of the charging station to achieve optimal charging and vehicle scheduling, and maximum profit of the EBs. Li et al. (2019) developed a formulation for the multi-depot vehicle scheduling problem with multiple vehicle types, ensuring that the number of buses would not exceed the capacity of the station. Tang et al. (2019) proposed both static and dynamic robust scheduling models for EBs to address the

challenges caused by the stochasticity of urban traffic conditions. Focusing on the availability of charging infrastructure, Olsen et al. (2020) developed a three-phase solution approach based on an aggregated time-space network for the EB vehicle scheduling problem. Liu and Ceder (2020) examined the EB vehicle scheduling problem with stationary battery chargers installed at transit terminal stations to minimize the total number of EBs. Alvo et al. (2021) introduced an exact solution approach for the EB scheduling problem with a mixed fleet of EBs and restricted number of chargers. Zhang et al. (2022) examined the multi-depot and multi-vehicle type EB scheduling problem by considering the parking restrictions of each depot. By considering the depot capacity constraint and partial recharging policy, Jiang et al. (2022) addressed a large-scale multi-depot EB scheduling problem.

Although many studies have been conducted on the subject of EB scheduling plan optimization, the EB charging facility sharing strategy with ECs has not been investigated. To develop a scheduling scheme optimization model for the EB route with a sharing strategy, the following three aspects should be considered: (i) optimization objectives include the terms of the charging revenues from ECs and the operating costs of the EB fleet when EB charging facility sharing schemes are applied; (ii) optimization variables are selected to model the availability of charging piles to EBs or ECs in each time period under the assumption that charging piles cannot be occupied by EBs and ECs within the same time period; and (iii) constraints are formulated to limit the start and end times of EB charging within a time period when it is charged using a charging pile.

1.3. Objectives and contributions

The main purpose of this study is to propose a collaborative optimization model to generate the vehicle scheduling scheme, charging scheme, and charging facility sharing scheme that would increase the charging revenues from ECs and relieve the charging facility shortage of ECs. The contributions of this study are as follows: (i) based on the charging facility sharing strategy, a collaborative optimization model is formulated with the objective of minimizing the operating costs of the EB route and waiting costs of ECs, and maximizing the charging revenues from ECs, to achieve optimal vehicle scheduling and charging facility sharing schemes; (ii) to address the nonlinearity of the formulated optimization model, an algorithm is developed to solve it by combining the enumeration method and branch and price; (iii) a real EB route is taken as an example to verify the effectiveness of the proposed optimization method, and a sensitivity analysis is conducted considering different contributing factors.

The remainder of this paper is organized as follows. Section 2 presents the calculation methods for the operating costs of EBs, waiting costs of ECs, and charging revenues from ECs, and establishes a vehicle scheduling model under the charging facility sharing strategy. Section 3 elaborates on an algorithm that combines the enumeration and branch and price to solve the problem. Section 4 displays a numerical example based on an actual bus route. The conclusions and potential extensions of the present work are discussed in Section 5.

2. Methodology

2.1. Problem description

Transit companies usually install a limited number of charging facilities at the departure station to facilitate the charging of EB fleets. The number of charging piles is S , which represents the maximum number of EBs that the station can serve at the same time. The whole-day operating hours are divided into Q ($q = 1, 2, \dots, Q$) time windows with identical electricity prices and departure intervals remaining in the same time window. The duration, start time, and end time of time window q are respectively denoted by τ_q , ST_q and ET_q . The charging facility sharing strategy allows charging piles of EBs to be utilized by ECs during certain time windows. The charging power for EBs is b (kW), and the average charging power for ECs is B (kW).

For an EB, a service trip is defined as the process in which it starts from the departure station, runs to the terminal, and then returns to the departure station. Let $K = \{k : k = 1, 2, \dots, K\}$ refers to the set of EBs. The set of scheduled daily service trips in the bus timetable is denoted by $I = \{i : i = 1, 2, \dots, I\}$, and the departure time of service trip i is D_i . The number of daily scheduled trips is jointly determined by the bus model and the passenger demand. A recharging trip is defined as the process where an EB gets recharged once, denoted by r , and the set of charging trips is denoted by $R = \{r : r = 1, 2, \dots, R\}$.

We assumed that the arrival of ECs to get charged follows the Poisson distribution (Bae and Kwasinski, 2011; Zhang and Li, 2015), of which the average arrival rate is λ_q^{car} (vehicle/h) in time window q . The mean electricity quantity that an EC needs to be replenished in time window q is $1/\mu_q^{car}$ (kWh), and the variance of that is σ_q^2 (kWh)². Because the battery rated capacity of an EC and the battery remaining power at the onset of charging have individual differences and are independent, the charging time of ECs (i.e., the service time of charging piles) is also independent and obeys the general distribution with a mean of $1/B\mu_q^{car}$ and a variance of σ_q^2/B^2 . In other words, it obeys a distribution in which the mean and variance exist and are known, but the specific function expression remains unknown. The departure station allows a maximum of $(H-S)$ ECs to queue for charging, following the first come first serve (FCFS) rule. H is the maximum number of vehicles that can be accommodated by the departure station.

As the charging piles can only be used by the EB or the EC in time window q , a binary decision variable $z_q \in \{0, 1\}$ is created to indicate the availability of charging piles to different types of vehicles in the time window q . To be specific, $z_q = 0$ represents that EBs are allowed to get charged in the time window q , and $z_q = 1$ indicates that ECs are allowed in the time window q . To optimize the departure times and end times of all service trips and charging trips of EB k , similarly to Rinaldi et al. (2020), let decision variable $x_{k,i}^t \in \{0, 1\}$ represent whether the service trip i is initiated by the EB k at time t . Let decision variable $y_{k,r}^t \in \{0, 1\}$ capture recharging

decisions, if the recharging trip r is initiated by EB k at time t , $y_{k,r}^t = 1$; otherwise $y_{k,r}^t = 0$.

Under the charging facility sharing strategy, public transit companies need to collaboratively optimize the EB vehicle scheduling scheme and charging facility sharing scheme, and the determination of the objective is an essential step in establishing the optimization model. First, the charging facility sharing strategy can increase the charging revenues of public transit companies and help the government to save subsidies. Second, the charging facility sharing strategy affects the charging scheme and number of EBs required for a route, which in turn affects the operating costs of the route (including vehicle acquisition costs and electricity expenses). Finally, the charging facility sharing strategy can affect the queuing time for the charging of ECs, and EC drivers typically expect shorter waiting times. Hence, we propose a collaborative optimization model with the objectives of minimizing the operating costs of the EB route and waiting costs of ECs, and maximizing the charging revenues from ECs, to optimize the availability of charging piles for different types of vehicles in each period and the service trips and charging trips performed by each EB per day.

2.2. Operating costs of the EB route

2.2.1. EB Battery remaining power estimation

Battery remaining power is an important parameter for the formulation of the model constraints and operating costs of the EB route. Theoretically, an EB can be arranged to get charged at any time when it idles between two service trips. To accurately calculate the available charging time and the change of battery remaining power, the time is discretized with a 1-min interval, and let $\mathbf{A} = \{t : t = 1, 2, \dots, \varpi\}$. ϖ is the end time of operating hours.

With the variables $x_{k,i}^t$ and $y_{k,r}^t$ defined in Section 2.1, the relationship between battery remaining power of EB k at times t and $t + 1$ can be expressed as Eq. (1):

$$W_k^{t+1} = W_k^t - \hat{w}_{k,i}^- \times x_{k,i}^t + \hat{w}_{k,r}^+ \times y_{k,r}^t \quad (1)$$

where W_k^t and W_k^{t+1} denote the battery remaining power of EB k at time t and $t + 1$, kWh; $\hat{w}_{k,i}^-$ is the estimated energy consumption of EB k in service trip i , kWh; $\hat{w}_{k,r}^+$ is the increased electricity quantity of EB k in recharging trip r , kWh.

As demonstrated by Eq. (1), when $x_{k,i}^t = 1$, the battery remaining power of EB k at any time t during the operation of service trip i ($T_{k,i}$) remains unchanged, which means that $W_k^{D_{k,i}} = W_k^{D_{k,i+1}} = \dots = W_k^{D_{k,i+T_{k,i}}} = W_k^{D_{k,i-1}} - \hat{w}_{k,i}^-$. Similarly, when $y_{k,r}^t = 1$, the battery remaining power of EB k at any time t during the charging time $T_{k,r}$ remains the same as its start time $ST_{k,r}$ on recharging trip r , which can be expressed as $W_k^{ST_{k,r}} = W_k^{ST_{k,r+1}} = \dots = W_k^{D_i+T_{k,r}} = W_k^{ST_{k,r-1}} + \hat{w}_{k,r}^+$. This estimation method of battery remaining power does not affect the final charging facility sharing scheme and vehicle scheduling scheme, but it does simplify the calculation.

(i) Energy consumption model for EBs

The energy consumption of EBs in each service trip is affected by multiple factors, such as travel time, curb mass, passenger mass, and ambient temperature. Based on the collected EB operation data, the weighted least squares (WLS) method is applied to establish an estimation model of trip energy consumption, as shown in Eq. (2).

$$\ln \hat{w}_{k,i} = \hat{v}_0 + \hat{v}_1 \ln L_i + \hat{v}_2 \ln \bar{m}_{k,i} + \hat{v}_3 \ln T_{k,i} + \hat{v}_4 |Tem_{k,i} - Tem_0| \quad (2)$$

where L_i is the mileage of trip i , km; $\bar{m}_{k,i}$ is the total mass of EB k on service trip i , kg; $Tem_{k,i}$ is the average ambient temperature of EB k during service trip i , °C; Tem_0 is the optimal working ambient temperature of the EB fleet, °C; $\hat{v}_0 \sim \hat{v}_4$ are the fitting coefficients.

The process of establishing Eq. (2) has been explained in another study (Ji et al., 2022) and is not repeated in this study for conciseness.

(ii) Charging model for EBs

To prolong battery life, it should be ensured that the battery SOC of EB k is always within the specified safety interval $[\delta_2, \delta_1]$ at any time. The increased electricity quantity obtained by EB k during the recharging trip has a linear relationship with recharging time, as shown in Eq. (3). The recharging time $T_{k,r}$ of EB k in the recharging trip r is determined jointly by the start time of recharging trip and the corresponding battery remaining power.

$$\hat{w}_{k,r}^+ = \frac{b}{60} T_{k,r} \quad (3)$$

$$T_{k,r} = \begin{cases} \min \left\{ ET_q^{bus} - ST_{k,r}, \frac{60}{b} \left(\delta_1 W_k^{rated} - W_k^{ST_{k,r}} - 1 \right), \frac{60}{b} \left(\delta_2 W_k^{rated} - \hat{W}_k^{end} \right) \right\} & \text{if } \hat{W}_k^{end} \leq \delta_2 W_k^{rated} \\ 0 & \text{if } \hat{W}_k^{end} > \delta_2 W_k^{rated} \end{cases} \quad (4)$$

$$q' = \frac{1}{2} (z_q + z_{q+1}) (1 + z_{q+1} - z_q) (1 - z_q \cdot z_{q+1}) q \quad \forall q \in \mathbf{Q} \quad (5)$$

where W_k^{rated} is the battery rated capacity of EB k , kWh; $W_k^{ST_{k,r}-1}$ represents the battery remaining power of EB k at time $ST_{k,r}-1$, kWh; \tilde{W}_k^{end} represents the battery remaining power of EB k at the end of operation without charging in the daytime, kWh; ET_q^{bus} is the end time of the recharging time window q' for EBs to which $ST_{k,r}$ belongs, $ET_q^{bus} > ST_{k,r}$. Time window q' is the last time window in a succession of time windows in which only EBs are allowed to charge, that is, the time window q when $z_q = 0$ and $z_{q+1} = 1$, as shown in Eq. (5). For example, if $z_3 = 0$, $z_4 = 0$, $z_5 = 0$, and $z_6 = 1$, then $q' = 5$.

2.2.2. Average daily acquisition costs

The average daily acquisition cost of the EB fleet is denoted as Z_1 , and can be calculated by Eq. (6). The calculation method for γ_k is displayed in Eq. (7), and is used to identify whether EB k is required by the operations of each day, $\sum_{k=1}^K \gamma_k \leq K$.

$$Z_1 = \sum_{k=1}^K \left(C_k \gamma_k \times \frac{\xi(1+\xi)^{Y_k}}{(1+\xi)^{Y_k} - 1} \right) \quad (6)$$

$$\gamma_k = 1 - \max \left\{ 1 - \sum_{t=0}^{\varpi} \sum_{i=1}^I x_{k,i}^t, 0 \right\} \quad (7)$$

where C_k is the unit acquisition cost of EB k , RMB; Y_k is the lifetime of EB k , day; ξ is the daily discount rate, %; $\sum_{t=0}^{\varpi} \sum_{i=1}^I x_{k,i}^t$ represents the number of service trips allocated to EB k during all-day operating hours. If EB k serves at least one trip for a day, $\max \left\{ 1 - \sum_{t=0}^{\varpi} \sum_{i=1}^I x_{k,i}^t, 0 \right\} = 0$.

2.2.3. Charging costs

A charging trip may last for several time windows. Let $T_{k,r,q}$ be the recharging time of the charging trip r of EB k in time window q . As shown in Eq. (9), $T_{k,r,q}$ is jointly determined by the start and end times of both recharging trip r and time window q . For any charging trip r , the relationship between $T_{k,r,q}$ and $T_{k,r}$ satisfies $T_{k,r} = \sum_{q=1}^Q T_{k,r,q}$. The total charging costs during the daily operating hours of the EB route is calculated as follows:

$$Z_2 = \frac{b}{60} \sum_{k=1}^K \sum_{r=1}^R \sum_{q=1}^Q (1 - z_q) C_q^l T_{k,r,q} \quad (8)$$

$$T_{k,r,q} = \min \{ ET_q, ST_{k,r} + T_{k,r} \} - \max \{ ST_q, ST_{k,r} \} \quad (9)$$

where C_q^l is the unit charging costs of EBs in time window q , which is equal to the electricity price of this time window, RMB/kWh.

2.3. Waiting costs of ECs

The recharging of ECs at the departure station can be regarded as a multi-server finite capacity queuing system ($M/G/S/H$), in which the arrival obeys a Poisson distribution, the recharging time follows a general service time distribution, the number of charging piles is S , and the departure station allows ECs to queue but does not allow queues to extend infinitely. When the total number of ECs in the system is H (including the ECs being charged), the newly arrived ECs are not allowed to enter the queuing system and are recommended to go to other dedicated charging depots for charging.

Traffic intensity $\rho_q = \frac{\lambda_q^{car}}{BS\rho_q^{car}}$ is used to indicate how busy the system is. According to Little's Law $E_q(L_{queue}) = \lambda_q^{car} E_q(T_{waiting})$, the average waiting time of ECs in time window q $E_q(T_{waiting})$ can be calculated by λ_q^{car} and the average queue length $E_q(L_{queue})$. In this study, the method in Kimura (1994) is adopted to estimate $E_q(L_{queue})$ and $E_q(T_{waiting})$, as expressed in Eqs. (10)-(11).

$$E_q(L_{queue}) = \sum_{j=S}^H (j - S) P_{q,j} = \frac{(S\rho_q)^S}{S!} \frac{\zeta}{(1 - \rho_q)(1 - \zeta)} \{ 1 - \zeta^{H-S} - (H - S)(1 - \zeta)\rho_q \zeta^{H-S-1} \} P_{q,0} \quad (10)$$

$$E_q(T_{waiting}) = \frac{1}{\lambda_q^{car}} \frac{(S\rho_q)^S}{S!} \frac{\zeta}{(1 - \rho_q)(1 - \zeta)} \{ 1 - \zeta^{H-S} - (H - S)(1 - \zeta)\rho_q \zeta^{H-S-1} \} P_{q,0} \quad (11)$$

where $P_{q,j}$ is the probability that there are j ECs in the system waiting to be recharged in time window q ; $P_{q,0}$ is the probability that there is no EC in the system waiting to be recharged in time window q .

$$P_{qj} = \begin{cases} \frac{(S\rho_q)^j}{j!} P_{q,0} & j = 0, \dots, S-1 \\ \frac{(S\rho_q)^S}{S!} \frac{1-\zeta}{1-\rho_q} \zeta^{j-S} P_{q,0} & j = S, \dots, H-1 \\ \frac{(S\rho_q)^S}{S!} \zeta^{H-S} P_{q,0} & j = H \end{cases} \quad (12)$$

$$P_{q,0} = \left[\sum_{j=0}^{S-1} \frac{(S\rho_q)^j}{j!} + \frac{(S\rho_q)^S}{S!} \frac{1-\rho_q \zeta^{H-S}}{1-\rho_q} \right]^{-1} \quad (13)$$

where $\zeta = \frac{\rho_q \Phi_G}{1-\rho_q} + \rho_q \Phi_G$, and Φ_G is the ratio of the average waiting time of queuing system $M/G/S$ to that of queuing system $M/M/S$ (Kong et al., 2015), as expressed by Eq. (14). In $M/G/S$, the arrival of ECs obeys the Poisson distribution, the recharging time follows the general distribution, and there are S charging piles, allowing infinite queuing. In $M/M/S$, the arrival of ECs obeys the Poisson distribution, the recharging time follows the negative exponential distribution, and there are S charging piles, allowing infinite queuing.

$$\Phi_G = \frac{E_q(T_{\text{waiting}}^{M/G/S})}{E_q(T_{\text{waiting}}^{M/M/S})} \quad (14)$$

where $E_q(T_{\text{waiting}}^{M/M/S})$ is the average waiting time in the $M/M/S$ queuing system, min; $E_q(T_{\text{waiting}}^{M/G/S})$ is the average waiting time in the $M/G/S$ queuing system, which can be approximately calculated using $E_q(T_{\text{waiting}}^{M/M/S})$ and the average waiting time of the $M/D/S$ queueing system $E_q(T_{\text{waiting}}^{M/D/S})$, as expressed by Eq. (15). In $M/D/S$, the arrival of ECs obeys the Poisson distribution, the recharging time follows the deterministic distribution, and there are S charging piles, allowing infinite queuing.

$$E_q(T_{\text{waiting}}^{M/G/S}) \approx \frac{1+n_S^2}{\frac{2n_S^2}{E_q(T_{\text{waiting}}^{M/M/S})} + \frac{1-n_S^2}{E_q(T_{\text{waiting}}^{M/D/S})}} \quad (15)$$

where n_S^2 is the squared coefficient of variance of charging time distribution, that is $(\sigma_q^2/B^2)^2$.

Combining Eqs. (9)-(15), we have the simplified expression of Φ_G as follows:

$$\Phi_G = \frac{(1+n_S^2)\Phi_D}{(2\Phi_D - 1)n_S^2 + 1} \quad (16)$$

where Φ_D is the ratio of $E_q(T_{\text{waiting}}^{M/D/S})$ to $E_q(T_{\text{waiting}}^{M/M/S})$, as shown in Eq. (17). After substituting Eqs. (17) - (19) into Eq. (16) (Wang et al., 2021; Zhu et al., 2022), it can be found that the value of Φ_G is only related to S and ρ_q .

$$\Phi_D = \frac{1}{2} \left[1 + F\left(\frac{S-1}{S+1}\right) f(\rho_q) \left(1 - \exp\left\{ -\frac{S-1}{(S+1)F\left(\frac{S-1}{S+1}\right)f(\rho_q)} \right\} \right) \right] \quad S \geq 1 \quad (17)$$

$$F\left(\frac{S-1}{S+1}\right) = \frac{S-1}{16S} \left(\sqrt{5S+4} - 2 \right) \quad (18)$$

$$f(\rho_q) = \frac{1-\rho_q}{\rho_q} \quad (19)$$

Vehicles are not allowed to queue in the last τ'_q min of the EC charging time window (a set of consecutive multiple time windows corresponding to $z_q = 1$), to ensure that all vehicles in the system have completed recharging and left by the end of EC charging time window. The waiting costs of ECs (Z_3) is the difference between the total waiting costs of ECs in all time windows of which $z_q = 1$ and the total waiting costs within τ'_q min before the end of each EC charging time window during the whole day's operation, as shown in Eqs. (20)-(21).

$$Z_3 = \frac{C_T}{60} \sum_{q=1}^Q \left[z_q \tau_q \lambda_q^{car} E_q(T_{\text{waiting}}) \right] - \frac{C_T}{60} \sum_{q=1}^Q \left[\tau'_q \lambda_{q''}^{car} E_{q''}(T_{\text{waiting}}) \right] \quad (20)$$

$$q'' = \frac{1}{2} (z_q + z_{q+1}) (1 + z_q - z_{q+1}) (1 - z_q \cdot z_{q+1}) q \quad \forall q \in Q \quad (21)$$

where C_T is the unit waiting time cost of ECs, RMB/vehicle/h; $\tau_q \lambda_q^{car}$ is the number of ECs recharged at the departure station in time window q , vehicle; $\lambda_{q''}^{car}$ is the average arrival rate of ECs in time window q'' , vehicle/h, $\lambda_0^{car} = 0$; $E_{q''}(T_{waiting})$ is the average waiting time of ECs in time window q'' , h, $E_0(T_{waiting}) = 0$. Time window q'' is the last time window of multiple consecutive windows, of which $z_q = 1$. For time window q'' , $z_q = 1$ and $z_{q+1} = 0$.

2.4. Charging revenues from ECs

Under the charging facility sharing strategy, the charging revenues consists of all service fees paid by ECs for using the EB charging facilities. Let τ_q'' be the shortest charging time of an EC, and the newly arrived car is not allowed to enter the departure station in the last τ_q'' min of the EC charging time window. Accordingly, the charging revenues from ECs during operation hours per day is:

$$Z_4 = \sum_{q=1}^Q \left[\frac{z_q}{60} C_0^2 \tau_q B \times \min \left\{ \frac{\lambda_q^{car}}{B \mu_q^{car}}, S \right\} \right] - \sum_{q=1}^Q \left[\frac{1}{60} C_0^2 \tau_q'' B \times \min \left(\frac{\lambda_q^{car}}{B \mu_q^{car}}, S \right) \right] \quad (22)$$

where C_0^2 is the unit service fee for ECs, RMB/kWh.

The first term on the right side of Eq. (22) is the sum of the average charging revenues from ECs in all time windows corresponding to $z_q = 1$ during the whole day's operation. The second term is the sum of the average charging revenues at the last τ_q'' min of each EC charging time window.

2.5. Model formulation

As described above, the objectives of the vehicle scheduling model under the charging facility sharing strategy are to minimize the average daily acquisition costs Z_1 and charging costs Z_2 of the EB route, minimize the waiting costs of ECs Z_3 , and maximize the charging revenues from ECs Z_4 . The objective function and constraints of the optimization model are listed in Eqs. (23) - (35).

$$\min Z = \alpha_1 Z_1 + \alpha_2 Z_2 + \alpha_3 Z_3 - \alpha_4 Z_4 \quad (23)$$

$$s.t. \quad \sum_{i=1}^I x_{k,i}' + \sum_{r=1}^R y_{k,r}' \leq 1 - a_k' \quad \forall k \in K, t \in A \quad (24)$$

$$x_{k,i}' + \frac{1}{T_{k,i} - 1} \sum_{\tilde{t}=D_{k,i}+1}^{D_{k,i}+T_{k,i}-1} \left(\sum_{i=1}^I x_{k,i} \tilde{t} + \sum_{r=1}^R y_{k,r} \tilde{t} \right) \leq 1 \quad \forall k \in K, i \in I, t \in A \quad (25)$$

$$y_{k,i}' + \frac{1}{T_{k,r} - 1} \sum_{\tilde{t}=ST_{k,r}+1}^{ST_{k,r}+T_{k,r}-1} \left(\sum_{i=1}^I x_{k,i} \tilde{t} + \sum_{r=1}^R y_{k,r} \tilde{t} \right) \leq 1 \quad \forall k \in K, r \in R, t \in A \quad (26)$$

$$\sum_{t=0}^{D_{k,i}} \sum_{i=1}^I x_{k,i}' = 0 \quad \forall k \in K \quad (27)$$

$$\sum_{t=0}^{\varpi} \sum_{k=1}^K x_{k,i}' = 1 \quad \forall i \in I \quad (28)$$

$$\sum_{k=1}^K \sum_{r=1}^R y_{k,r}' \leq S \quad \forall t \in A \quad (29)$$

$$T_{k,r} \geq T_{min} \quad \forall k \in K, r \in R \quad (30)$$

$$ET_{q''} - ET_{\tilde{q}} \geq \beta \quad \forall q \in Q \quad (31)$$

$$x_{k,i}' - \frac{W_k'}{\widehat{W}_{k,i} + \delta_2 W_k^{rated}} \leq 0 \quad \forall k \in K, i \in I, t \geq D_{k,i} \quad (32)$$

$$W_k^0 = \delta_1 W_k^{rated} \quad \forall k \in K \quad (33)$$

$$x_{k,i}' \in \{0, 1\}, y_{k,r}' \in \{0, 1\} \quad \forall k \in K, i \in I, r \in R \quad (34)$$

$$z_q \in \{0, 1\} \quad \forall q \in Q \quad (35)$$

The objective function is expressed by Eq. (23), where $\alpha_1, \alpha_2, \alpha_3$, and α_4 are weighting coefficients and $\alpha_1 + \alpha_2 + \alpha_3 + \alpha_4 = 1$. Constraint (24) indicates that at most one service trip or one recharging trip can be assigned to EB k when $a_k^t = 0$. State identifier $a_k^t \in \{0, 1\}$, $a_k^t = 1$ means that EB k is not available for any service trip at time t ; otherwise $a_k^t = 0$. Constraint (25) indicates that after service trip i is assigned to EB k , no more service trips or recharging trips can be assigned to it during the travel time of service trip i . $D_{k,i}$ represents the scheduled departure times of EB k on trip i . Constraint (26) restricts no more service trips or recharging trips that can be assigned to EB k before finishing the current charging trip r . Constraint (27) represents that EB k is forbidden from departing in advance for trip i . Constraint (28) means that service trip i needs to be served by one EB. Constraint (29) indicates that at most S EBs can be recharged simultaneously at any time t , which can avoid the queue of EBs at the charging piles. Constraint (30) sets the shortest charging time limit for EBs. We encourage the types of vehicles that are allowed to be charged in multiple consecutive time windows to be the same as possible, that is, as shown in Eq. (31), the difference between the end times of any EC charging time windows q'' and its adjacent EB charging time windows \tilde{q}' should be no shorter than β for the whole day's operation. This would lead to the extension of recharging time of EBs to meet the need of subsequent trips and the reduction of drivers' burden to remember the opening hours of charging facilities. Constraint (32) indicates that EB k will not be assigned to service trip i with insufficient battery remaining power, which is set to guarantee the integrity of service trips. The battery SOC of EB k is defined to be δ_1 at the start time ($t = 1$) of the daily operation in Constraint (33). Constraints (34) and (35) show the value ranges of the decision variables.

3. Solution algorithm

The model established in this paper is a nonlinear integer programming problem, which is NP-hard. It contains numerous binary

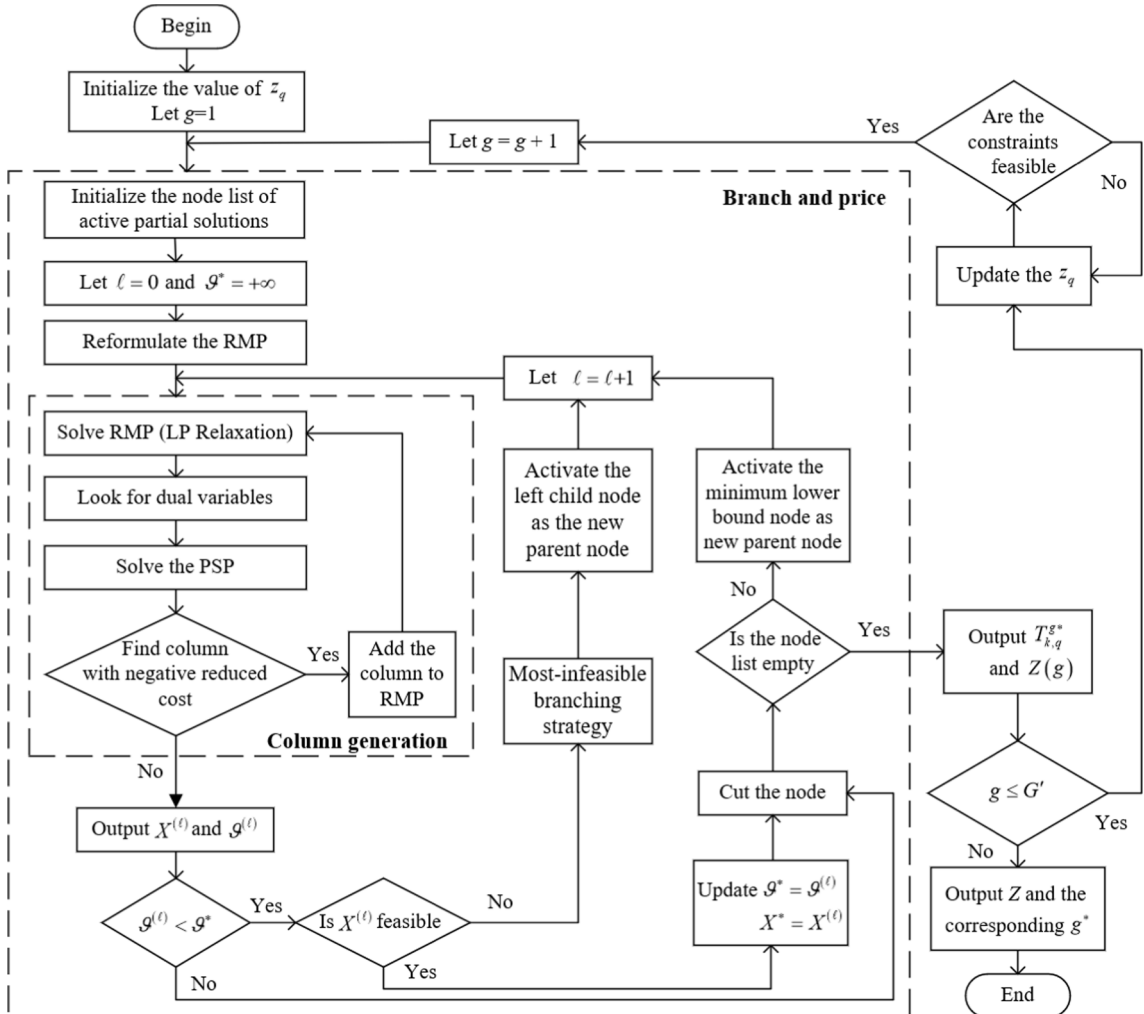


Fig. 1. Flowchart of the algorithm.

variables, and it is time consuming to apply the branch and bound (B&B) algorithm for optimal solution searching of the proposed model. To reduce the scale of the decision variables and speed up the solution searching process, the column generation (CG) algorithm is incorporated in the B&B algorithm to solve the restricted relaxation model, which is called the branch and price algorithm (B&P).

As described in Section 2, charging costs Z_2 is jointly affected by variables $x_{k,i}^t, y_{k,r}^t$, and z_q . A nonlinear relationship exists between Z_2 and the three variables. This causes difficulty in decomposing the original problem into a restricted master problem (RMP) and a series of pricing sub-problems (PSP) using the column generation algorithm. Compared to the vehicle and charging scheduling schemes, the charging facility sharing scheme has relatively limited feasible alternatives. Thus, we design an algorithm that combines enumeration and B&P to solve the optimization model formulated in Section 2.5. To apply this algorithm, the original problem is reformulated into a charging facility sharing problem and a vehicle and charging scheduling problem for EBs, as shown in Sections 3.1 and 3.2. Specifically, a feasible charging facility sharing scheme is first given, and the corresponding vehicle and charging scheduling problem is then solved using the B&P algorithm. Subsequently, the feasible charging facility sharing scheme is continuously updated by enumeration, and the costs Z under different charging schemes are calculated. Finally, the charging facility sharing scheme with the lowest cost and the corresponding vehicle and charging scheduling scheme are output as the optimal solution. A flowchart of the algorithm is presented as Fig. 1.

3.1. Optimal charging facility sharing scheme using enumeration

As described in Section 2.1, the operation hours are divided into Q time windows per day. Accordingly, 2^Q charging facility sharing schemes can be generated. In practice, however, all EBs need to serve on the route during the morning and evening peak hours, with no opportunity to get charged. Therefore, the availability of charging facilities during peak hours can only be assigned to ECs. With this constraint, the remaining number of feasible alternatives for the charging facility sharing scheme is denoted as G' .

The optimization model of the charging facility sharing scheme is extracted from the original model, as shown in Eqs. (36) - (39).

$$\min Z = \min\{Z(1), Z(2), \dots, Z(g), \dots, Z(G')\} \quad (36)$$

$$Z(g) = \alpha_3 Z_3^g - \alpha_4 Z_4^g + \alpha_2 \sum_{q=1}^Q \sum_{k=1}^K C_q^1 (1 - z_q) T_{k,q}^{g*} + \alpha_1 Z_1^g \quad (37)$$

$$ET_{q''} - ET_q \geq \beta \quad \forall q \in Q \quad (38)$$

$$z_q \in \{0, 1\} \quad \forall q \in Q \quad (39)$$

where $Z(g)$ is the total cost of the g -th charging facility sharing scheme, $RMB, 1 \leq g \leq G'; Z_3^g, Z_4^g$, and Z_1^g are the waiting costs of ECs, charging revenues from ECs, and average daily acquisition costs of the EB route under the g -th charging facility sharing scheme, respectively, RMB ; $T_{k,q}^{g*}$ represents the optimal charging duration of EB k in the time window q under the g -th charging scheme, min. Eq. (38) is the same as constraint (31) in the original problem, and Eq. (39) provides the value ranges for the decision variables.

3.2. Vehicle and charging scheduling based on B&P

3.2.1. Column generation algorithm

In the CG algorithm, we first use the Dantzig-Wolfe decomposition to reformulate the original scheduling problem into an RMP and PSP. Then the RMP is solved to obtain the minimum operating costs of the EB route. The relevant dual variables are achieved to solve the PSP, and new EB scheduling and charging schemes are searched for and obtained. Finally, a column with the negative reduced cost is added to the RMP to solve it iteratively.

(i) Restricted master problem (RMP)

We define a variable $\varepsilon_{\theta(k)} \in \{0, 1\}$, if and only if the vehicle scheduling and charging scheme of EB k $\theta(k)$ is used to solve the RMP $\varepsilon_{\theta(k)} = 1$; otherwise, $\varepsilon_{\theta(k)} = 0, \theta(k) \in \widehat{\varphi}(k) \subseteq \varphi(k)$. Here, $\varphi(k)$ is the set of all possible vehicle scheduling and charging schemes for EB k , and $\widehat{\varphi}(k)$ is a subset of $\varphi(k)$. The vehicle and charging scheduling problems are reformulated into the following RMP model:

$$\min \sum_{k=1}^K \sum_{\theta(k)=1}^{\widehat{\varphi}(k)} C_{\theta(k)}^g \varepsilon_{\theta(k)} \quad (40)$$

$$s.t. \quad \sum_{k=1}^K \sum_{\theta(k)=1}^{\widehat{\varphi}(k)} \sum_{r=0}^m x_{k,r}^t \varepsilon_{\theta(k)} = 1 \quad \forall i \in I \quad (41)$$

$$\sum_{\theta(k)}^{\widehat{\varphi}(k)} \varepsilon_{\theta(k)} \leq 1 \quad \forall k \in K \quad (42)$$

$$\sum_{k=1}^K \sum_{\theta(k)}^{\widehat{\varphi}(k)} \sum_{r=1}^R y_{k,r}^t \varepsilon_{\theta(k)} \leq S \quad \forall t \in A \quad (43)$$

$$0 \leq \varepsilon_{\theta(k)} \leq 1 \quad \forall k \in K, \theta(k) \in \widehat{\varphi}(k) \quad (44)$$

Objective function (40) minimizes the operating costs of the EB route. $C_{\theta(k)}^g$ is the charging costs of $\theta(k)$ under the g -th charging facility sharing scheme, RMB, and can be calculated by substituting the charging plan corresponding to the scheme $\theta(k)$ into Eq. (8) and Eq. (9). Constraint (41) is formulated to ensure that each service trip i be assigned to an EB throughout the operating hours in all feasible schemes. Constraint (42) is set to ensure that each EB can adopt only one vehicle and charging scheduling scheme. Constraint (43) limits the number of EBs charged simultaneously at any time t within the capacity of the charging depot. Constraint (44) provides the value ranges of the decision variables after LP relaxation.

(ii) Pricing sub-problems (PSP)

The PSP is used to find the optimal vehicle and charging scheduling scheme with a negative reduced cost to be added to the $\widehat{\varphi}(k)$ of the RMP. In each iteration of the column generation process, K pricing subproblems need to be solved. An optimal vehicle and charging scheduling scheme is generated for the pricing problem of EB k , but only the optimal scheme with a negative reduced cost (as shown in Eq. (45)) is added to the RMP. This means that at most K columns need to be added to the RMP in each iteration of the column generation process. The PSP is formulated as follows.

$$\min C_{\theta(k)}^g - \sum_{i=1}^I \sum_{t=0}^{\overline{t}} x_{k,i}^t \pi_i + \sum_{r=1}^R \sum_{t=0}^{\overline{t}} y_{k,r}^t \pi_t + \pi_k \quad (45)$$

$$s.t. \quad \sum_{t=0}^{D_{k,i}} \sum_{i=1}^I x_{k,i}^t = 0 \quad (46)$$

$$\sum_{i=1}^I x_{k,i}^t + \sum_{r=1}^R y_{k,r}^t \leq 1 - a_k^t \quad \forall t \in A \quad (47)$$

$$x_{k,i}^t + \frac{1}{T_{k,i} - 1} \sum_{\tilde{t}=D_{k,i}+1}^{D_{k,i}+T_{k,i}-1} \left(\sum_{i=1}^I x_{k,i}^{\tilde{t}} + \sum_{r=1}^R y_{k,r}^{\tilde{t}} \right) \leq 1 \quad \forall i \in I, t \in A \quad (48)$$

$$y_{k,i}^t + \frac{1}{T_{k,r} - 1} \sum_{\tilde{t}=ST_{k,r}+1}^{ST_{k,r}+T_{k,r}-1} \left(\sum_{i=1}^I x_{k,i}^{\tilde{t}} + \sum_{r=1}^R y_{k,r}^{\tilde{t}} \right) \leq 1 \quad r \in R, t \in A \quad (49)$$

$$T_{k,r} \geq T_{\min} \quad \forall r \in R \quad (50)$$

$$x_{k,i}^t - \frac{W_k^t}{\widehat{W}_{k,i}} + \delta_2 W_k^{rated} \leq 0 \quad \forall i \in I, t \geq D_{k,i} \quad (51)$$

$$W_k^0 = \delta_1 W_k^{rated} \quad (52)$$

$$x_{k,i}^t \in \{0, 1\}, y_{k,r}^t \in \{0, 1\} \quad \forall i \in I, r \in R \quad (53)$$

where π_i , π_t , and π_k are the dual variables of Constraints (41), (43), and (42) in the RMP problem, respectively.

3.2.2. Branch and price algorithm

After applying the CG algorithm, the solutions of the RMP after LP relaxation are usually non-integer and infeasible. The B&P algorithm should be performed on non-integer solutions to find the optimal integer solution. The steps of the B&P algorithm are as follows:

Step 0: Define the initial column set $\psi = \bigcup_{k \in K} \widehat{\varphi}(k)$, take the feasible vehicle and charging scheduling scheme set as the root node of the tree, and put it into the node list of active partial solutions that are currently required to be branched. Let X^* be the current optimal feasible solution and ϑ^* be the corresponding optimal objective function value.

Step 1: Let the number of iterations $\ell = 0$ and $\vartheta^* = +\infty$.

Step 2: Obtain the RMP of the current parent node using the CG algorithm described in Section 3.2.1. The optimal solution and

objective function value of the current parent node are denoted by $X^{(\ell)}$ and $\vartheta^{(\ell)}$, respectively.

If $\vartheta^{(\ell)} < \vartheta^*$ and $X^{(\ell)}$ is not feasible for the original problem, go to Step 3.

If $\vartheta^{(\ell)} < \vartheta^*$ and $X^{(\ell)}$ is feasible for the original problem, update $\vartheta^* = \vartheta^{(\ell)}$ and $X^* = X^{(\ell)}$, cut the node, and go to Step 4.

If $\vartheta^{(\ell)} \geq \vartheta^*$, cut the node and go to Step 4.

Step 3: Branch the current parent node further into two child nodes based on the most infeasible branching rule.

Step 3.1: If any variable $e_{\theta(k)}$ in the current optimal solution does not satisfy the 0–1 integer constraint, select the variable whose score $\eta_{k,i} = \sum_{\theta(k)=1}^{\widehat{\varphi}(k)} \sum_{t=0}^m x_{k,i}^t e_{\theta(k)}^*$ ($e_{\theta(k)}^*$ is the optimal solution of RMP) is the closest to 0.5. Note that if more than one variable meets the requirement, we randomly choose one of them.

Step 3.2: Formulate two constraints: $e_{\theta(k)} = 1$ (left child node) and $e_{\theta(k)} = 0$ (right child node) based on EB k and service trip i , which are added to the current node PSP, respectively. The left child node requires that service trip i must be run by EB k , and the right child node requires that service trip i must be run by other EBs.

Step 3.3: To ensure compatibility between branch constraints and pricing problems, delete all columns in the RMP that assign service trip i to other electric buses and all columns where EB k does not run service trip i for the left child node and delete all columns from the RMP where EB k runs service trip i for the right child.

Step 3.4: Based on the Depth-First Search Rule, activate the left child node as the new parent node and let $\ell' = \ell + 1$. Add the right child node to the current node list, set its lower limit to be $\vartheta^{(\ell')}$, and return to Step 2.

Step 4: If the current node list which needs to be branched also contains nodes, select the node with the smallest lower bound in the node list based on the Best-First Search Rule, and set it as the current parent node. Let $\ell' = \ell + 1$, and return to Step 2. If the node list that currently needs to branch is empty, terminate the algorithm and output the ϑ^* and corresponding X^* .

4. Numerical example

4.1. Real data preparation

We take EB route 203 in Meihekou, Jilin Province, China as an example to verify and analyze the established optimization method. The departure station of Route 203 is located near the Hailong Lake Scenic Area, which has a high demand for EC charging and sufficient land resources to set charging facilities. The route connects Hailong Lake and the railway station whose mileage is 12 km ($L = 24$ km) and $N = 13$ stations, as shown in Fig. 2.

An EB that departs from Hailong Lake, travels to the railway station, and then returns to Hailong Lake is considered a complete service trip. The first and last service trips are scheduled to depart at 6:10 and 21:00, respectively. The dispatching headway for peak hours including 7:00–9:00 and 16:00–18:00 is 5 min, and that for off-peak hours is 10 min. A total of 114 service trips are conducted throughout the operation hours per day. The average ambient temperature during operation hours is -24.1°C (January 7, 2021). Let $\beta = 120$ min, and the whole-day operating hours are divided into 9 time windows considering time-of-day tariffs and timetables, which are demonstrated in Table 1, along with the unit charging cost of the EBs in each time window. To guarantee that the SOC of each EB reaches δ_1 before operation, charging facilities are available only to the EBs in the ninth time window (23:00–5:00), $z_9 = 0$. As analyzed in Section 3.1, during peak hours, charging facilities are available only to ECs, $z_2 = z_6 = 1$. On this basis, a total of 64 feasible charging facility sharing schemes can be generated, namely $G' = 64$.

There are 20 EBs available, namely $K = 20$, which are powered by LiFePO₄ batteries. The battery rated capacity of all EBs are homogenous with the W_k^{rated} of 130 kWh and specific energy of 140.40 Wh/kg. The specified battery SOC safety interval is [20%, 90%], that is $\delta_2 = 20\%$, $\delta_1 = 90\%$. The minimum charging time $T_{\min} = 5$ min. All EBs were purchased in May 2020 in full with no loans, and the warranty period is 8 years, i.e., $\xi = 0$ and $Y_k = 2920$ days. Bus curb mass and rated passenger load are 7300 kg and 60 people,

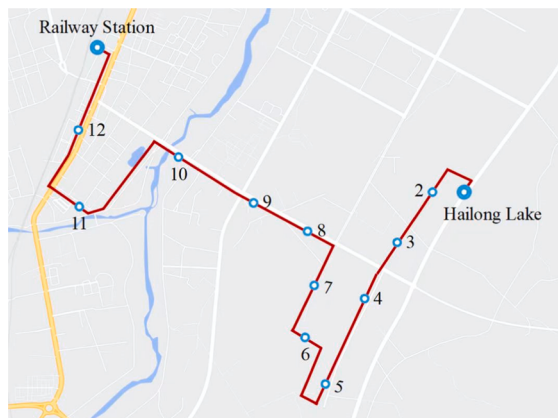


Fig. 2. Sketch diagram of EB route 203 in Meihekou, Jilin Province, China.

Table 1

Dispatching headway and unit charging cost of EBs in each time window.

q	ST_q	ET_q	τ_q (min)	h_q (min)	C_q^l (RMB/kWh)
1	5:00	7:00	120	10	0.33
2	7:00	9:00	120	5	0.63
3	9:00	11:00	120	10	0.63
4	11:00	14:00	180	10	0.94
5	14:00	16:00	120	10	0.63
6	16:00	18:00	120	5	0.63
7	18:00	21:00	180	10	0.94
8	21:00	23:00	120	—	0.63
9	23:00	5:00	360	—	0.33

respectively.

We collected the actual data of 2,200 trips from June 2020 to June 2021, each of which included license plate number, date, route mileage, departure time, travel time, battery SOC, average ambient temperature, and energy consumption. The model expressed in Eq. (2) in Section 2.2.1 is fitted by the actual data using the WLS, and the result is shown in Eq. (54). The optimal working ambient temperature of the model is 23.7 °C, and the mean absolute percentage error (MAPE) is 11.73%.

$$\ln \hat{w}_{k,i} = -8.091 + 0.553 \ln L_i + 0.780 \ln \bar{m}_{k,i} + 0.353 \ln T_{k,i} + 0.008 |T_{k,i} - 23.7| \quad (54)$$

A charging depot with 6 charging piles ($S = 6$) is set up at Hailong Lake. The number of ECs allowed for queuing in depot $H-S = 4$. Under the charging facility sharing strategy, the charging power of EBs $b = 60$ kW, and the average charging power of ECs $B = 30$ kW. The unit price of the EC service fee in all time windows q during operation hours $C_0^2 = 0.80$ RMB/kWh. The arrival rate and charging demand of ECs in each time window near the scenic area of Hailong Lake are displayed in Table 2. We assume that Z_1, Z_2, Z_3 , and Z_4 are equally important for policymakers, and their weighting coefficients are all set to 0.25. The other important input parameters of the model are listed in Table 3.

4.2. Baseline results

We use Java programming and CPLEX Optimizers V12.6.3 to solve the model established in this paper. Numerical experiments were performed on a computer with a 2.90 GHz CPU and 16 GB RAM under Windows 10, and the optimal solution was found within 3460 s. The optimal total costs $Z = 652.775$ RMB, including the average daily acquisition costs of the EB route $Z_1 = 3,397.3$ RMB, the total charging costs of the EB route $Z_2 = 630.8$ RMB, the waiting costs of ECs $Z_3 = 420.6$ RMB, and the charging revenues from ECs $Z_4 = 1837.5$ RMB.

The departure time of the first trip (6:10) and end time of the last trip (22:00) are set as the start and end times of the optimization, denoted as $t \in [0, 950]$. The optimal vehicle scheduling and charging scheme of the EB fleet considering the charging facility sharing strategy is recorded as Scheme A, as shown in Fig. 3. When all time windows are available only to the EBs, which means that $z_q = 0$ ($q = 1, 2, \dots, 9$), the optimal vehicle and charging scheduling scheme obtained from the proposed model is recorded as Scheme B, as depicted in Fig. 4. In both Fig. 3 and Fig. 4, yellow bars refer to the service trips, blue bars with diagonal patterns denote recharging trips, and white bars represent the idle time between trips.

In Scheme A, charging piles are available to the EB fleet in time windows 5 and 9. The ECs can get charged in other time windows. Besides, 16 EBs are arranged to operate on this route, and the energy consumption of the EB fleet for daily operation is 1668.2 kWh. The charging depot is idle for approximately 259 min throughout operation hours per day, mainly in time windows 4, 5, and 7.

In Scheme B, the charging scheme of the EBs is mainly distributed in time windows 3 and 5. The total costs of Scheme B is $Z = 1002.85$ RMB, including the average daily acquisition costs of the EB route $Z_1 = 3,397.3$ RMB (16 EBs) and the charging costs of the EB route $Z_2 = 614.2$ RMB. The charging depot is idle for 862 min throughout the operation hours per day, and the idle time durations in time windows 3 and 5 are 98 min and 120 min, respectively.

The number of service trips that each EB needs to serve (ξ_k), starting time of charging (ST_k), depth of charge (DOC_k), and remaining

Table 2

Arrival rate and charging demand of ECs in each time window.

q	λ_q^{car} (vehicle/h)	$1/\mu_q^{car}$ (kWh/h)	σ_q^2 (kWh 2 /h 2)	$E_q(T_{waiting})$ (min)
1	7	31.6	10.2	27.3
2	18	21.0	13.9	11.6
3	15	23.6	11.0	14.3
4	4	28.0	8.2	5.6
5	14	25.9	8.2	12.9
6	13	28.9	11.1	16.0
7	3	34.1	10.4	6.6
8	5	38.9	13.3	36.9

Table 3

Other important input parameters in the model.

Notation	Value	Unit	Notation	Value	Unit
τ'_q	10	min	C_k	620,000	RMB
τ''_q	30	min	C_T	12	RMB/h

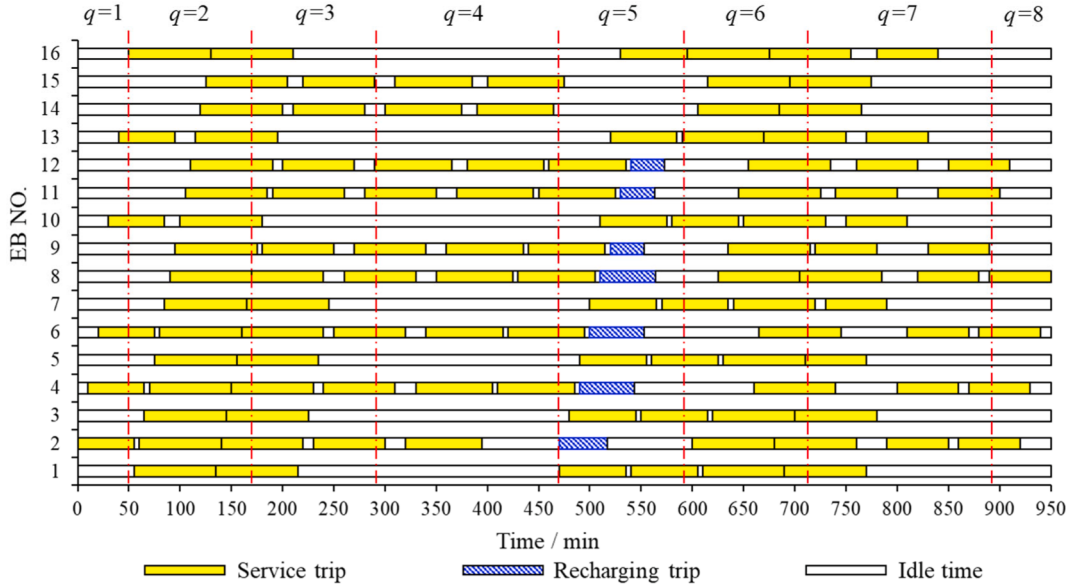


Fig. 3. Optimal EB vehicle and charging scheduling scheme under charging facility sharing strategy.

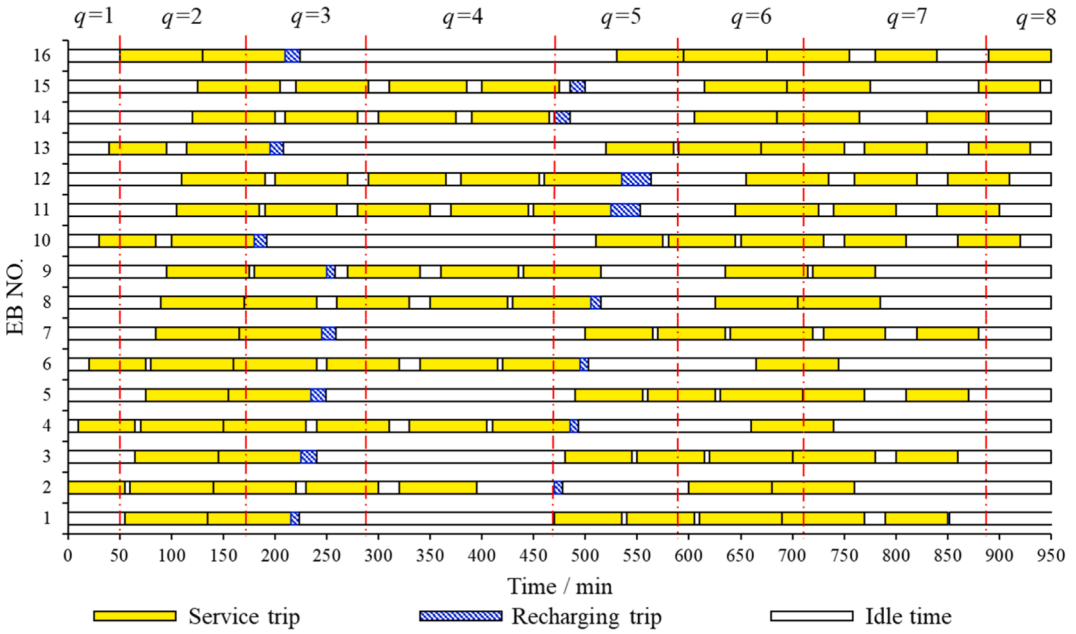


Fig. 4. Optimal EB vehicle scheduling and charging scheme without sharing charging facilities.

battery power at the end of operation (W_k^{end}) in Scheme A and Scheme B are shown in Table 4.

It is observed that the fleet sizes and average daily acquisition costs in Scheme A and Scheme B are identical to the results presented above. The charging costs of the EB route is composed of daytime and overnight charging costs. These two costs in Scheme A are 168.6

Table 4

Comparison between Scheme A and Scheme B.

k	Scheme A				Scheme B			
	ξ_k	ST_k	$DOC_k(\%)$	$W_k^{end}(\text{kWh})$	ξ_k	ST_k	$DOC_k(\%)$	$W_k^{end}(\text{kWh})$
1	6	–	–	31.3	7	9:45	6.10	26.0
2	9	14:00	31.60	26.0	7	14:00	6.19	26.0
3	6	–	–	31.3	7	9:55	11.18	26.0
4	9	14:20	36.38	26.0	7	14:15	5.89	26.0
5	6	–	–	32.7	7	10:05	10.08	26.0
6	9	14:30	36.38	26.0	7	14:25	5.89	26.0
7	6	–	–	32.7	7	10:15	5.98	26.0
8	9	14:40	37.56	26.0	7	14:35	7.07	26.0
9	8	14:50	21.22	26.0	7	10:20	10.08	26.0
10	6	–	–	34.6	7	9:10	8.65	26.0
11	8	15:00	21.22	26.0	8	14:55	21.22	26.0
12	8	15:10	21.49	26.0	8	15:05	21.49	26.0
13	6	–	–	33.5	7	9:25	9.46	26.0
14	6	–	–	30.8	7	14:00	11.56	26.0
15	6	–	–	30.8	7	14:16	11.56	26.0
16	6	–	–	31.8	7	9:40	10.80	26.0

RMB and 462.2 RMB, respectively, and those in Scheme B are 133.7 RMB and 480.5 RMB. Compared to Scheme B, the charging costs in Scheme A has a slight increment of 16.6 RMB and there is an additional waiting costs of ECs, which is 420.6 RMB. But the charging revenues from ECs is up to 1837.5 RMB, which is sufficient to recover the loss.

The charging scheme of Scheme A is arranged in one time window, whereas that of Scheme B is arranged in two time windows. It is difficult to arrange charging trips for all EBs in one time window while maintaining normal operation of the EB route. Thus, only part of the EB fleet is arranged to get recharged during operation hours in Scheme A, and the battery SOC of the remaining EBs after completing daily operation is still no lower than 20%. In Scheme B, on the other hand, each EB is arranged to get recharged during operation hours, and the battery SOC of all buses after daily operation remains at 20%. With the fixed daily energy consumption of the EB fleet, Scheme B makes better use of the lower overnight electricity price, which leads to a lower charging cost. However, it is not valid to determine whether Scheme B is better than Scheme A. As stated in Section 2.4, newly arrived ECs in the last τ_q'' min of the charging time window for ECs are not allowed to get charged in the charging depot. This indicates that more charging time windows for ECs result in more invalid charging time as well as more losses in charging revenues. We take an example by adjusting the charging time window for EBs from 14:00–16:00 to 10:00–11:00 and 15:00–16:00. In this situation, the charging time available and unit charging costs for EBs remain unchanged, while the number of charging time windows for ECs increases from 2 to 3, causing a reduction of 99.2 RMB in charging revenues from ECs. Therefore, the vehicle and charging scheme in Scheme A is more beneficial for cost savings under the charging facility sharing strategy.

4.3. Sensitivity analyses

Based on the vehicle scheduling model formulated in Section 2.5 under the charging facility sharing strategy, sensitivity analyses

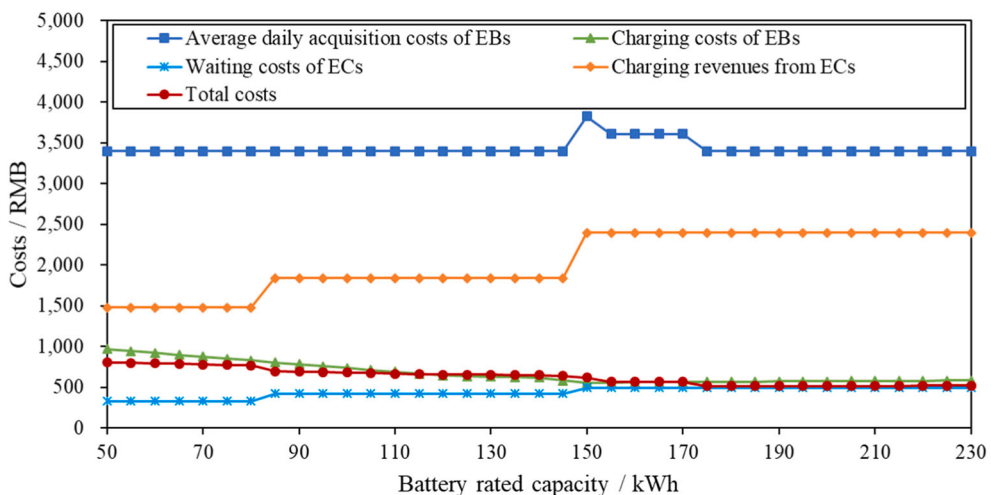


Fig. 5. Relationship curve between battery rated capacity and costs.

are conducted on multiple input parameters, including the battery rated capacity of EBs, ambient temperature during operation, number of charging piles in the charging depot, and charging demand of ECs.

(i) Battery rated capacity of EBs

Battery rated capacity of EBs is an important factor affecting operating costs of EBs. With a fixed battery specific energy, battery rated capacity has a linear relationship with battery mass. Hence, battery rated capacity has impacts on the bus curb mass and daily energy consumption, which finally affects the operating costs of the EBs. In the current market, battery rated capacities of most EBs are over 50 kWh. It is also assumed that the EB fleet serving the route is homogeneous. When other input parameters remain unchanged, the variation range of battery rated capacity is divided by a 5-kWh interval, and the average daily acquisition costs of EBs, charging costs of EBs, waiting costs of ECs, charging revenues from ECs, and total costs under each battery rated capacity are obtained and illustrated in Fig. 5.

When $W_k^{\text{rated}} \in [50 \text{ kWh}, 80 \text{ kWh}]$, 16 EBs are required and two charging time windows are arranged for the EBs during operation hours. The waiting costs of ECs and charging revenues from ECs are 327.7 RMB and 1477.5 RMB, respectively. With the increase in battery rated capacity, the daytime charging time of EBs shrinks, and the charging costs of EBs gradually decrease at an average rate of 4.7 RMB/kWh.

When $W_k^{\text{rated}} \in [85 \text{ kWh}, 145 \text{ kWh}]$, 16 EBs are required and one charging time window is arranged for EBs during operation hours. The waiting costs of ECs and charging revenues from ECs are 420.6 RMB and 1837.5 RMB, respectively. With the increase in battery rated capacity, the daytime charging time of the EBs also shrinks, and the charging costs of EBs gradually decrease at an average rate of 3.7 RMB/kWh.

When $W_k^{\text{rated}} \geq 150 \text{ kWh}$, EBs only get charged overnight and no daytime charging is arranged, which means that time windows, except time window 9, are available only to ECs ($z_q = 1, q = 1, 2, \dots, 8$). Compared with the scenario when $W_k^{\text{rated}} = 145 \text{ kWh}$, two more EBs need to be purchased when $W_k^{\text{rated}} = 150 \text{ kWh}$, and the average daily acquisition costs increase by 424.6 RMB. However, an additional 559.6 RMB in charging revenues from ECs can be obtained. With the increase in battery rated capacity, the driving range of each EB also increases, allowing each bus to serve more trips during the daytime without being recharged. Therefore, when W_k^{rated} is increased from 150 kWh to 170 kWh, the number of required EBs is reduced to 17 to save the average daily acquisition costs. When W_k^{rated} is increased to 175 kWh, 16 EBs are sufficient to ensure normal operation of the route without charging during the daytime. In general, increasing the battery rated capacity results in a gradual stepwise decrease in total costs, which reaches a minimum when no daytime charging for EBs is arranged and the battery rated capacity is sufficient for operational requirements.

(ii) Ambient temperature during operation

Ambient temperature is another important factor that influences the daily energy consumption and operating costs of EBs. In the data collection, the minimum and maximum ambient temperatures were -27.0°C and 35.0°C , respectively. With the required fleet size under the lowest ambient temperature and other input parameters introduced in Section 4.1, the temperature range is divided by a 3.1°C interval. Fig. 6 depicts the daily energy consumption and charging costs of the EBs under different ambient temperatures, while Fig. 7 depicts the costs of daytime and overnight charging.

As shown in Fig. 6, when the ambient temperature exceeds the optimal working ambient temperature, the daily energy consumption and charging costs of EBs gradually rise at an increasing rate, with the increase of the ambient temperature. When the

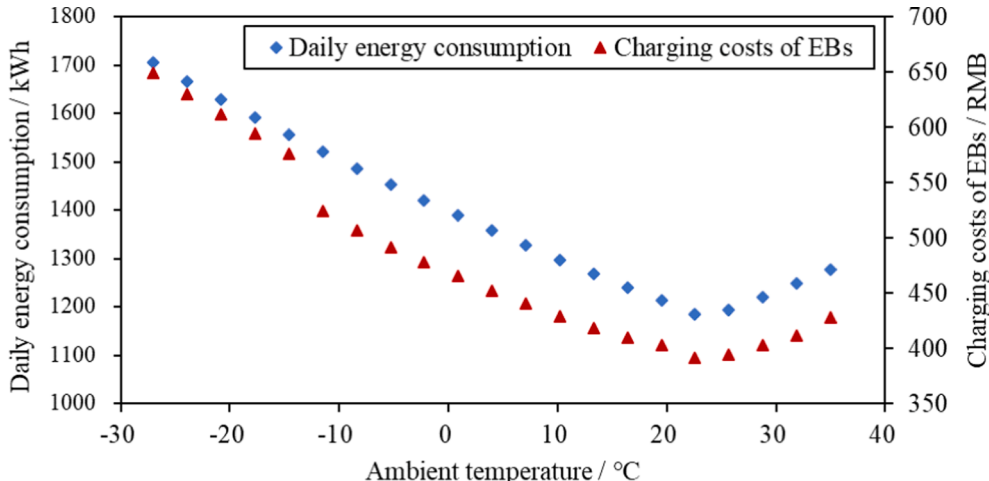


Fig. 6. Daily energy consumptions and charging costs of EBs under different ambient temperatures.

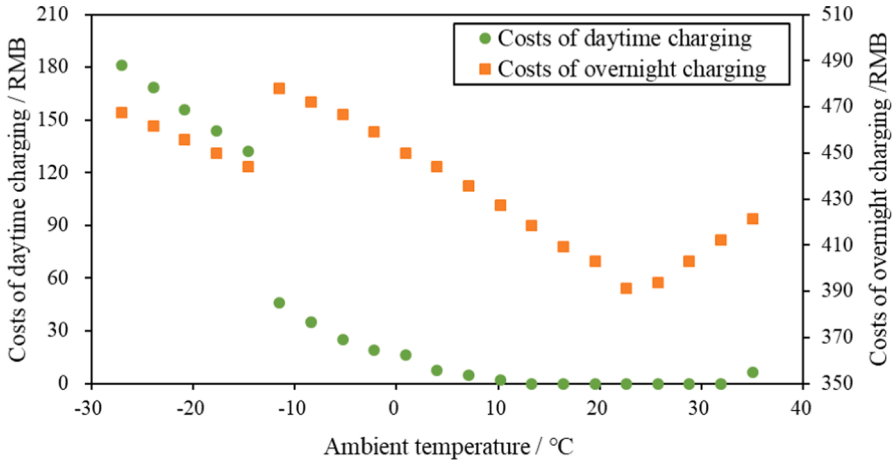


Fig. 7. Costs of daytime and overnight charging under different ambient temperatures.

ambient temperature is below the optimal working ambient temperature, the daily energy consumption and charging costs of EBs gradually increase with the decrease of the ambient temperature. During the temperature dropping from -11.5°C to -14.6°C , the number of charging time windows for EBs remains unchanged, the number of EBs which are arranged to get recharged in the daytime is reduced from 8 to 7, the daytime charging time is extended from 73 min to 159 min, and the overnight charging time is narrowed from 1448 min to 1397 min. Therefore, the costs of daytime charging increases from 45.8 RMB to 132.1 RMB, and the costs of overnight charging decreases from 477.9 RMB to 444.3 RMB. Accordingly, the total charging costs soars from 523.7 RMB to 576.4 RMB.

When the ambient temperature is below 13.3°C or over 31.9°C , the EB fleet should be arranged to get recharged in the daytime. The daytime charging time and charging costs increase with the increase of temperature during the former temperature range and with the decrease of the temperature during the latter range. Only one charging time window is scheduled for EBs. When the ambient temperature ranges between 13.3°C and 31.9°C , the EB fleet has no need to be recharged in the daytime, and the daytime charging cost remains 0 accordingly.

Under the effects of ambient temperature, considerable differences exist in daily energy consumptions and charging costs of EBs among different seasons. Therefore, without changing the EB fleet size, the vehicle and charging scheduling scheme should be updated every season or every month, based on fluctuations in the ambient temperature.

(iii) Number of charging piles

The number of charging piles directly affects the waiting time of ECs and the charging revenues from ECs. The number also affects the charging scheduling scheme because it constrains the number of EBs which can be charged simultaneously in the charging depot,

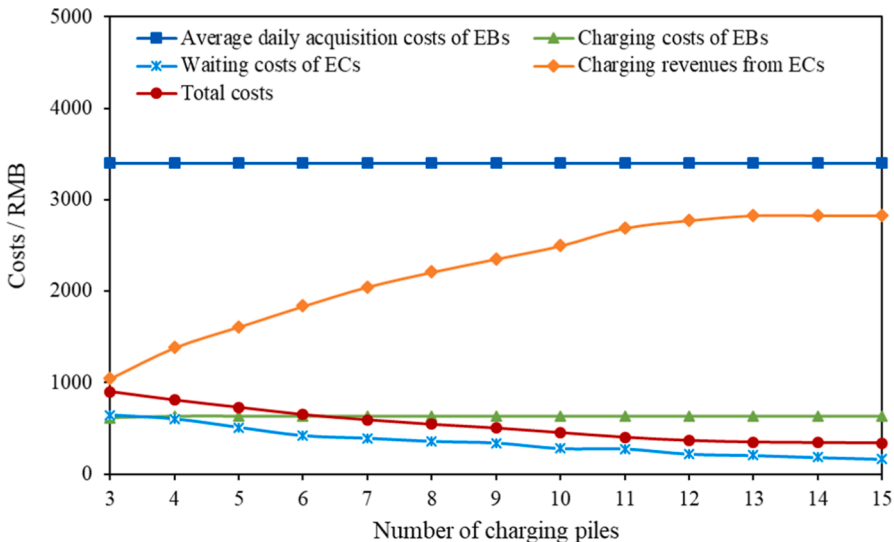


Fig. 8. Relationship curve between the number of charging piles and costs.

and further affects the vehicle scheduling scheme. With all other input parameters illustrated in Section 4.1, the average daily acquisition costs of EBs, charging costs of EBs, waiting costs of ECs, charging revenues from ECs, and total costs with different numbers of charging piles are obtained and illustrated in Fig. 8.

When the number of charging piles varies from 3 to 15, the average daily acquisition costs of the EBs remains the same at 3397.3 RMB, and 16 EBs are arranged to operate per day. When 3 charging piles are set up, time windows 3 and 5 are available only to the EBs, and the charging costs of EBs is 614.2 RMB. When 4 charging piles are placed, time window 5 is available only to the EBs and the charging costs of EBs is 630.8 RMB.

Under the charging demand of ECs as shown in Table 2, the waiting costs of ECs decrease from 645.3RMB to 164.6RMB by 74% with an increase in the number of charging piles. Besides, the charging revenues increase and total costs decrease with an increase in the number of charging piles. The total cost tends to level off when the number of charging piles reaches over 13. The charging revenues rise from 1044 RMB to 2775.2 RMB by 61.2% when the number of charging piles increased from 3 to 12. When this number reaches 13 or more, the charging demands of the ECs in all time windows are satisfied, leading to a constant cost of 2829.2 RMB.

The utilization rate of charging piles in time window q for EBs or ECs is denoted by ρ'_q . If the availability of charging piles in time window q is arranged to ECs ($z_q = 1$), we have $\rho'_q = 1$ when the traffic intensity $\rho_q > 1$ and $\rho'_q = \rho_q$ when $\rho_q \leq 1$. If the availability of charging piles in time window q is arranged to EBs ($z_q = 0$), ρ'_q equals to the ratio of the total charging time of the whole EB fleet to τ_q . The utilization rate under each time window throughout the operation hours per day is shown in Fig. 9.

When 3 charging piles are set up, the utilization rates in time windows 3 and 5 are 76.1% and 82.8%, respectively, and those in other time windows are 100%. When 4 charging piles are set up, the utilization rates in time windows 4, 5, and 7 begin to decrease, and those in other time windows are still 100%. When there are 7, 8, and 12 charging piles, the utilization rates in time windows 8, 1, and 3 start to decrease, respectively, and those in time windows 2 and 6 are still 100%. When the number of charging piles increases to 13, the utilization rates in time windows 2 and 6 begin to decrease. Since the electricity prices in time windows 4 and 7 are relatively high, the charging demands are accordingly lower, resulting in a low utilization rate of charging piles. Taking into account the utilization of charging facilities in different time windows, the daily comprehensive utilization rate is calculated with τ_q as the weight, and the rates are 95.4%, 91.5%, 84.3%, 79.5%, 75.3%, 70.6%, 66.4%, 63.1%, 60.4%, 58.0%, 54.5%, 50.6%, and 47.2%, respectively, under different numbers of charging piles from 3 to 15. In a real-world implementation, the optimal number of charging piles can be jointly determined by considering the costs and utilization rate of charging facilities, based on the charging demands of EBs and ECs.

(iv) Charging demand of ECs

The charging demand of the ECs determines the charging revenues from ECs. When 6 charging piles are placed in the charging depot, time window 3 is taken as an instance to analyze the charging revenues and utilization rates of charging piles under different arrival rates and average electricity quantity needs of ECs, as shown in Fig. 10 and Fig. 11.

With the increase in the arrival rate and average electricity quantity needs of ECs, the charging revenues and utilization rates gradually rise and level off at 288 RMB and 100%. In addition, the higher the arrival rate and average electricity quantity needed, the earlier the charging revenue and utilization rate reach stable values. When the charging revenue is less than 288 RMB and the utilization rate is lower than 100%, linear growth of the charging revenues and utilization rates to the arrival rate is observed with a fixed average electricity quantity needs of ECs. On the other hand, with a fixed arrival rate, linear growth of the charging revenues and utilization rates to the average electricity quantity needs is observed as well.

5. Conclusions

This study proposes a nonlinear integer programming model for vehicle scheduling problems under a charging facility sharing strategy, with constraints on the service integrity and capacity of the charging depot. The objective function of the optimization model is to minimize the average daily acquisition and charging costs of the EB route, waiting costs of the ECs, and to maximize the charging revenues from the ECs. The availability of each time window for different vehicle types and the service and charging trips arranged to each EB per day are defined as the optimization variables for the model. A hybrid algorithm combining enumeration and branch and price algorithm is designed to solve the formulated model. A numerical example is conducted on an actual EB route for the analysis and validation. The conclusions of this study are as follows:

- (i) The proposed optimization method for vehicle scheduling problems under the charging facility sharing strategy is able to adjust charging facility sharing and vehicle scheduling schemes without changing the timetable of the route, improving the utilization rate of charging facilities, alleviating the charging difficulty of ECs, and increasing the charging revenues of public transit companies from ECs.
- (ii) With an increase in the battery rated capacity of EBs, the daytime charging demand decreases. Hence, EB charging facilities can be shared with ECs to increase the revenues of public transit companies and reduce government subsidies. Batteries with higher rated capacity, however, usually bring about heavier battery mass and bus curb mass, leading to the increase in daily energy consumption of EBs and accordingly higher operating costs of the EB route.
- (iii) The total energy consumption of EBs and the charging demand of ECs are jointly considered in the proposed model, making it applicable to the same route in different seasons or other EB routes by providing optimal alternatives of charging facility sharing scheme, vehicle and charging scheduling scheme for EBs.

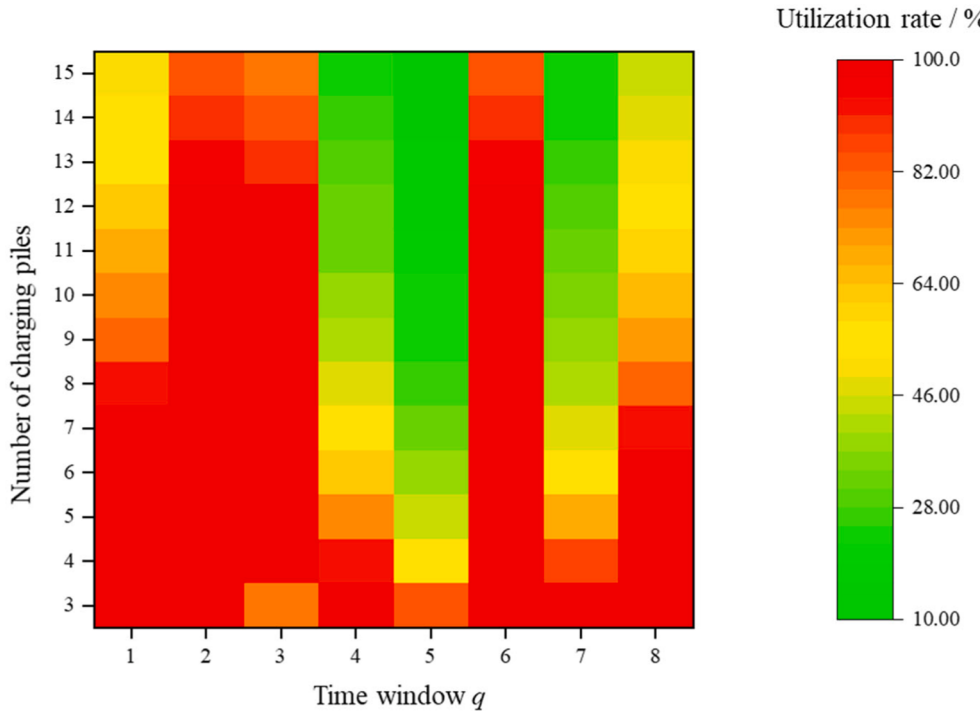


Fig. 9. Utilization rates of charging piles under different number of charging piles.

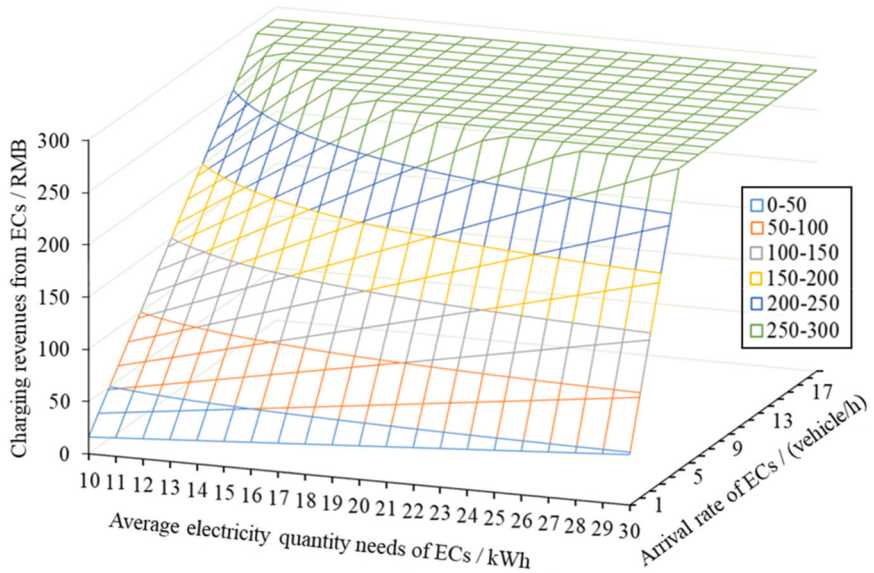


Fig. 10. Charging revenues under different arrival rates and average electricity quantity needs of ECs.

One strong assumption of this study is that the service fee and arrival rate of the ECs are fixed. However, the arrival rate varies with changes in the service fees. A future research direction is to model the charging selection of ECs and incorporate then into the optimization model.

CRediT authorship contribution statement

Jinhua Ji: Conceptualization, Writing – original draft. **Yiming Bie:** Supervision, Conceptualization, Methodology, Writing – review & editing. **Linhong Wang:** Methodology, Validation, Resources, Supervision, Writing – review & editing.

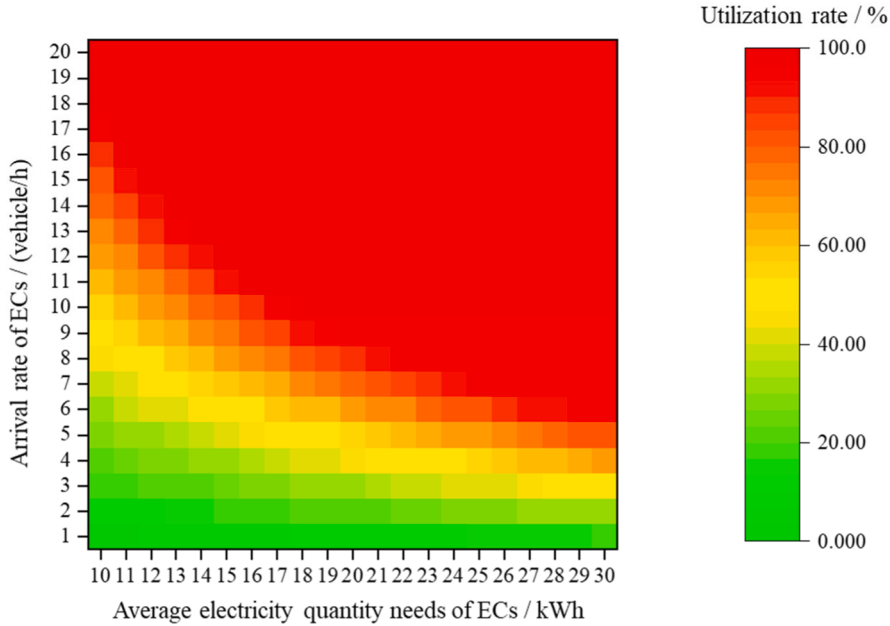


Fig. 11. Utilization rates of charging piles under different arrival rates and average electricity quantity needs of ECs.

Declaration of Competing Interest

The authors declare that they have no known competing financial interests or personal relationships that could have appeared to influence the work reported in this paper.

Data availability

Data will be made available on request.

Acknowledgment

This work was supported in part by the Key Project of National Natural Science Foundation of China [grant numbers 52131203 & 52220105001], China Postdoctoral Science Foundation [grant numbers 2019M661214 & 2020T130240], and Fundamental Research Funds for the Central Universities [grant number 2020-JCXY-40].

Appendix A. Outline of notation

Sets	
$k \in K$	Set of EBs
$i \in I$	Set of scheduled daily service trips in the bus timetable
$r \in R$	Set of charging trips
$t \in A$	Set of operating times
$q \in Q$	Set of time windows
Variables	
$z_q \in \{0, 1\}$	Availability of charging piles to different types of vehicles in the time window q
$x_{k,i}^t \in \{0, 1\}$	Whether the service trip i is initiated by the EB k at time t
$y_{k,r}^t \in \{0, 1\}$	Whether the recharging trip r is initiated by EB k at time t
Parameters	
S	Number of charging piles in depot
H	Maximum number of vehicles that can be accommodated in depot
b	Charging power for EBs (kW)
B	Average charging power for ECs (kW)
λ_q^{car}	Average arrival rate of ECs to get charged (vehicle/h).
$1/\mu_q^{car}$	Average electricity quantity that an EC replenished in time window q (kWh)
σ_q^2	Variance of electricity quantity that an EC replenished in time window q (kWh) ²

(continued on next page)

(continued)

D_i	Departure time of the service trip i
W_k^{rated}	Battery rated capacity of EB k (kWh)
W_k^t	Battery remaining power of EB k at time t (kWh)
$\widehat{W}_{k,i}$	Estimated energy consumption of EB k in service trip i (kWh)
$\widehat{W}_{k,r}^+$	Increased electricity quantity of EB k in recharging trip r (kWh)
$T_{k,r}$	Recharging time of EB k in the recharging trip r (min)
$T_{k,r,q}$	Recharging time of the charging trip r of EB k in time window q (min)
$T_{k,i}$	Travel time of EB k in service trip i (min)
$ST_{k,r}$	Time of EB k starting the recharging trip r
ST_q	Start time of time window q
ET_q	End time of time window q
ET_q^{bus}	End time of the time window q' for EB recharging to which $ST_{k,r}$ belongs
τ_q	Duration of time window q (min)
τ'_q	Time that vehicles are not allowed to queue in time window q (min)
τ''_q	Time that newly arrived car is not allowed to enter depot in time window q (min)
$E_q(T_{\text{waiting}})$	Average waiting time of ECs in time window q (min)
$E_q(L_{\text{queue}})$	Average queue length of ECs in time window q (vehicle)

References

- Abdelwahed, A., van den Berg, P.L., Brandt, T., Collins, J., Ketter, W., 2020. Evaluating and optimizing opportunity fast-charging schedules in transit battery electric bus networks. *Transp. Sci.* 54 (6), 1601–1615.
- An, K., 2020. Battery electric bus infrastructure planning under demand uncertainty. *Transport. Res. Part C-Emerging Technol.* 111, 572–587.
- Alvo, M., Angulo, G., Klapp, M.A., 2021. An exact solution approach for an electric bus dispatch problem. *Transport. Res. E-Log* 156, 102528.
- Bae, S., Kwasinski, A., 2011. Spatial and temporal model of electric vehicle charging demand. *IEEE Trans. Smart Grid* 3 (1), 394–403.
- Bie, Y.M., Hao, M.J., Guo, M.Z., 2021a. Optimal electric bus scheduling based on the combination of all-stop and short-turning strategies. *Sustainability* 13 (4), 1827.
- Bie, Y.M., Ji, J.H., Wang, X.Y., Qu, X.B., 2021b. Optimization of electric bus scheduling considering stochastic volatilities in trip travel time and energy consumption. *Comput. Aided Civ. Inf. Eng.* 36 (12), 1530–1548. <https://doi.org/10.1111/mice.12684>.
- Ceder, A., 2011. Public-transport vehicle scheduling with multi vehicle type. *Transport. Res. Part C-Emerging Technol.* 19 (3), 485–497.
- Coretti Sanchez, N., Martinez, I., Alonso Pastor, L., Larson, K., 2022. On the simulation of shared autonomous micro-mobility. *Commun. Transport. Res.* 2, 100065.
- Deng, R.L., Liu, Y., Chen, W.Z., Liang, H., 2021. A survey on electric buses-energy storage, power management, and charging scheduling. *IEEE Trans. Intell. Transp. Syst.* 22 (1), 9–22.
- Dirks, N., Schiffer, M., Walther, G., 2022. On the integration of battery electric buses into urban bus networks. *Transport. Res. Part C-Emerging Technol.* 139, 103628.
- Estrada, M., Mension, J., Salicru, M., Badia, H., 2022. Charging operations in battery electric bus systems considering fleet size variability along the service. *Transport. Res. Part C-Emerging Technol.* 138, 103609.
- Gao, Y.J., Guo, S.X., Ren, J.F., Zhao, Z., Ehsan, A., Zheng, Y.A., 2018. An electric bus power consumption model and optimization of charging scheduling concerning multi-external factors. *Energies* 11 (8), 2060.
- Gkiotsalitis, K., 2021. Bus holding of electric buses with scheduled charging times. *IEEE Trans. Intell. Transp. Syst.* 22 (11), 6760–6771.
- Global Mass Transit Report, 2021. Electric buses in the US: New administration to focus on zero-emission fleet. <https://reglobal.co/electric-buses-in-the-us-new-administration-to-focus-on-zero-emission-fleet/> (Accessed May 10, 2021).
- Hall, C.H., Ceder, A., Ekstrom, J., Quttineh, N.H., 2019. Adjustments of public transit operations planning process for the use of electric buses. *J. Intell. Transp. Syst.* 23 (3), 216–230.
- He, Y., Liu, Z.C., Song, Z.Q., 2020. Optimal charging scheduling and management for a fast-charging battery electric bus system. *Transport Res E-Log* 142, 102056.
- Hu, H., Du, B., Liu, W., Pereza, P., 2022. A joint optimisation model for charger locating and electric bus charging scheduling considering opportunity fast charging and uncertainties. *Transport. Res. Part C: Emerging Technol.* 141, 103732.
- Huang, D., Wang, S., 2022. A two-stage stochastic programming model of coordinated electric bus charging scheduling for a hybrid charging scheme. *Multimodal Transportation* 1 (1), 100006.
- Huang, D., Wang, Y.R., Jia, S., Liu, Z.Y., Wang, S.A., 2022. A Lagrangian relaxation approach for the electric bus charging scheduling optimisation problem. *Transportmetrica A*, (in press), DOI: 10.1080/23249935.2021.2023690.
- Ji, J., Bie, Y., Zeng, Z., Wang, L., 2022. Trip energy consumption estimation for electric buses. *Commun. Transport. Res.* 2, 100069.
- Jiang, M.Y., Zhang, Y., Zhang, Y., 2022. A branch-and-price algorithm for large-scale multidepot electric bus scheduling. *IEEE Transactions on Intelligent Transportation Systems*, (in press), DOI: 10.1109/TITS.2022.3165876.
- Kimura, T., 1994. Approximations for multi-server queues: System interpolations. *Queueing Systems Theory Appl.* 17 (3–4), 347–382.
- Kong, C., Bayram, I.S., Devetsikiotis, M., 2015. Revenue optimization frameworks for multi-class PEV charging stations. *IEEE Access* 3, 2140–2150.
- Lajunen, A., 2014. Energy consumption and cost-benefit analysis of hybrid and electric city buses. *Transport. Res. Part C-Emerging Technol.* 38, 1–15.
- Leou, R.C., Hung, J.J., 2017. Optimal charging schedule planning and economic analysis for electric bus charging stations. *Energies* 10 (4), 483.
- Li, B.D., Chen, Y., Wei, W., Huang, S.W., Xiong, Y.F., Mei, S.W., Hou, Y.H., 2021. Routing and scheduling of electric buses for resilient restoration of distribution system. *IEEE Trans. Transp. Electrif.* 7 (4), 2414–2428.
- Li, J.Q., 2014. Transit bus scheduling with limited energy. *Transp. Sci.* 48 (4), 521–539.
- Li, J.Q., 2016. Battery-electric transit bus developments and operations: A review. *Int. J. Sustain. Transp.* 10 (3), 157–169.
- Li, L., Lo, H.K., Xiao, F., Cen, X.K., 2018. Mixed bus fleet management strategy for minimizing overall and emissions external costs. *Transport. Res. Part D-Transport Environ.* 60, 104–118.
- Li, L., Lo, H.K., Xiao, F., 2019. Mixed bus fleet scheduling under range and refueling constraints. *Transport. Res. Part C-Emerging Technol.* 104, 443–462.
- Li, X.H., Wang, T.Z., Li, L.J., Feng, F.Y., Wang, W., Cheng, C., 2020. Joint optimization of regular charging electric bus transit network schedule and stationary charger deployment considering partial charging policy and time-of-use electricity prices. *J. Adv. Transp.* 2020, 1–16.
- Liu, T., Ceder, A., 2020. Battery-electric transit vehicle scheduling with optimal number of stationary chargers. *Transport. Res. Part C-Emerging Technol.* 114, 118–139.
- Liu, X.H., Qu, X.B., Ma, X.L., 2021a. Optimizing electric bus charging infrastructure considering power matching and seasonality. *Transport. Res. Part D-Transport Environ.* 100, 103057.
- Liu, X.H., Qu, X.B., Ma, X.L., 2021b. Improving flex-route transit services with modular autonomous vehicles. *Transport Res E-Log* 149, 102331.

- Liu, Z.C., Song, Z.Q., 2017. Robust planning of dynamic wireless charging infrastructure for battery electric buses. *Transport. Res. Part C-Emerging Technol.* 83, 77–103.
- Ma, X.L., Zhong, H.Y., Li, Y., Ma, J.Y., Cui, Z.Y., Wang, Y.H., 2021. Forecasting transportation network speed using deep capsule networks with nested LSTM models. *IEEE Trans. Intell. Transp. Syst.* 22 (8), 4813–4824.
- Meng, Q., Liu, P., Liu, Z.Y., 2022. Integrating multimodal transportation research. *Multimodal Transportation* 1 (1), 100001.
- Olsen, N., Kliwer, N., Wolbeck, L., 2020. A study on flow decomposition methods for scheduling of electric buses in public transport based on aggregated time-space network models. *CEJOR* 30, 883–919.
- Paul, T., Yamada, H., 2014. Operation and charging scheduling of electric buses in a city bus route network, *IEEE 17th International Conference on Intelligent Transportation Systems (ITSC)*. IEEE, Qingdao, P. R. China, pp. 2780–2786.
- Pelletier, S., Jabali, O., Mendoza, J.E., Laporte, G., 2019. The electric bus fleet transition problem. *Transport. Res. Part C-Emerging Technol.* 109, 174–193.
- Perumal, S.S.G., Lusby, R.M., Larsen, J., 2022. Electric bus planning & scheduling: A review of related problems and methodologies. *Eur. J. Oper. Res.* 301 (2), 395–413.
- Qu, X., Wang, S., Niemeier, D., 2022. On the urban-rural bus transit system with passenger-freight mixed flow. *Commun. Transport. Res.* 2, 100054.
- Rinaldi, M., Picarelli, E., D'Ariano, A., Viti, F., 2020. Mixed-fleet single-terminal bus scheduling problem: Modelling, solution scheme and potential applications. *Omega* 96, 102070.
- Rogge, M., van der Hurk, E., Larsen, A., Sauer, D.U., 2018. Electric bus fleet size and mix problem with optimization of charging infrastructure. *Appl. Energy* 211, 282–295.
- Sustainable Bus, 2020. Electric bus, main fleets and projects around the world. <https://www.sustainable-bus.com/electric-bus/electric-bus-public-transport-main-fleets-projects-around-world/> (Accessed May 19, 2020).
- Tang, X.D., Lin, X., He, F., 2019. Robust scheduling strategies of electric buses under stochastic traffic conditions. *Transport. Res. Part C-Emerging Technol.* 105, 163–182.
- Teng, J., Chen, T., Fan, W., 2020. Integrated approach to vehicle scheduling and bus timetabling for an electric bus line. *J. Transport. Engineering Part A-Syst.* 146 (2), 04019073.
- Teoh, L.E., Khoo, H.L., Goh, S.Y., Chong, L.M., 2018. Scenario-based electric bus operation: A case study of Putrajaya, Malaysia. *Int. J. Transp. Sci. Technol.* 7 (1), 10–25.
- Wang, G., Fang, Z.H., Xie, X.Y., Wang, S., Sun, H.J., Zhang, F., Liu, Y.H., Zhang, D.S., 2021a. Pricing-aware real-time charging scheduling and charging station expansion for large-scale electric buses. *ACM Trans. Intell. Syst. Technol.* 12 (1), 1–26.
- Wang, J., Kang, L.X., Liu, Y.Z., 2020. Optimal scheduling for electric bus fleets based on dynamic programming approach by considering battery capacity fade. *Renew. Sustain. Energy Rev.* 130, 109978.
- Wang, S., Chen, X., Qu, X., 2021b. Model on empirically calibrating stochastic traffic flow fundamental diagram. *Commun. Transport. Res.* 1, 100015.
- Wang, Y.S., Huang, Y.X., Xu, J.P., Barclay, N., 2017. Optimal recharging scheduling for urban electric buses: A case study in Davis. *Transport Res E-Log* 100, 115–132.
- Yildirim, S., Yildiz, B., 2021. Electric bus fleet composition and scheduling. *Transport. Res. Part C-Emerging Technol.* 129, 103197.
- Yue, L., Abdel-Aty, M., Wang, Z., 2022. Effects of connected and autonomous vehicle merging behavior on mainline human-driven vehicle. *J. Intelligent Connected Vehicles* 5 (1), 36–45.
- Zhang, A.J., Li, T.Z., Zheng, Y., Li, X.F., Abdullah, M.G., Dong, C.Y., 2022a. Mixed electric bus fleet scheduling problem with partial mixed-route and partial recharging. *Int. J. Sustain. Transp.* 16 (1), 73–83.
- Zhang, L., Li, Y., 2015. Optimal management for parking-lot electric vehicle charging by two-stage approximate dynamic programming. *IEEE Trans. Smart Grid* 8 (4), 1722–1730.
- Zhang, L., Wang, S., Qu, X., 2021. Optimal electric bus fleet scheduling considering battery degradation and non-linear charging profile. *Transport Res E-Log* 154, 102445.
- Zhang, L., Zeng, Z., Gao, K., 2022b. A bi-level optimization framework for charging station design problem considering heterogeneous charging modes. *J. Intelligent Connected Vehicles* 5 (1), 8–16.
- Zhu, J., Tasic, I., Qu, X., 2022. Flow-level Coordination of Connected and Autonomous Vehicles in Multilane Freeway Ramp Merging Areas. *Multimodal Transportation* 1 (1), 100005.
- Zhou, G.J., Xie, D.F., Zhao, X.M., Lu, C.R., 2020. Collaborative optimization of vehicle and charging scheduling for a bus fleet mixed with electric and traditional buses. *IEEE Access* 8, 8056–8072.
- Zhou, Y., Meng, Q., Ong, G.P., 2022. Electric bus charging scheduling for a single public transport route considering nonlinear charging profile and battery degradation effect. *Transport. Res. Part B-Methodological* 159, 49–75.